Reduction of Multiple Hits in Atom Probe Tomography

M. Thuvander[1]*, A. Kvist[1], L.J.S. Johnson[2], J. Weidow[1] and H.-O. Andrén[1]

1. Chalmers University of Technology, Göteborg, Sweden
2. Linköping University, Linköping, Sweden

*corresponding author: mattias.thuvander@chalmers.se

Abstract

The accuracy of compositional measurements using atom probe tomography is often reduced because some ions are not recorded when several ions hit the detector in close proximity to each other and within a very short time span. In some cases, for example in analysis of carbides, the multiple hits result in a preferential loss of certain elements, namely those elements that frequently field evaporate in bursts or as dissociating molecules. In this paper a method of reducing the effect of multiple hits is explored. A fine metal grid was mounted a few millimeters behind the local electrode, effectively functioning as a filter. This resulted in a decrease in the overall detection efficiency, from 37% to about 5%, but also in a decrease in the fraction of multiple hits. In an analysis of tungsten carbide the fraction of ions originating from multiple hits decreased from 46% to 10%. As a result, the measured carbon concentration increased from 48.2 at.% to 49.8 at.%, very close to the expected 50.0 at.%. The characteristics of the multiple hits were compared for analyses with and without the grid filter.

Keywords: atom probe tomography, multiple hits, detection efficiency, quantification, carbides, tungsten carbide

1. Introduction

Atom probe tomography (APT) is a very versatile tool for measuring local compositions on a nanometer scale. The method relies on identifying and positioning individual ions being field evaporated from the tip of a needle-shaped sample. The detection efficiency is usually 30-60%, depending on instrument type, and it is the same for all elements, thus giving excellent compositional accuracy, without the need of standard samples and element specific calibration. In some cases, though, the accuracy of concentration measurements is significantly reduced, for example when analyzing carbides [1], nitrides [2], silicides [3] or semiconductors [4]. In the case of carbides, the main reason why the obtained carbon concentration is usually too low is the limited capability of the detector to register all ions resulting from the same pulse. The ions have a strong tendency of being field evaporated in bursts, which results in several ions hitting the detector in close proximity to each other and within a very short time span. The fraction of carbon ions in these multiple hit events is higher than expected from the concentration, leading to a preferential loss of carbon in the analysis. The dead time of the detector together with the efficiency of the process to resolve multiple hits are the factors governing the severity of the effect. Detectors have been designed for improved multiple hit detection [5], but they are slower and more expensive than the detectors of most commercial instruments.

One way to limit the influence of the detector dead time on the measured carbon concentration in analysis of carbides is to decrease the mass resolution, as demonstrated for 1D atom probe by Zackrisson et al. [6]. However, their approach, to introduce a spread in flight path, can hardly be adapted to 3D APT. In some cases it is possible to use only isotopes of low abundance for quantification, as the probability is low that more than one such ion from a single pulse hit the detector. This has been demonstrated for the analysis of carbides, using the ^{13}C isotope [1]. To some extent it is possible to decrease the fraction of multiple events by changing the analysis conditions. When using laser pulsing the fraction decreases slightly if the laser pulse energy is increased, as shown for Ti(C, N) [7].

The nature of the detected multiple events has recently been investigated by Yao et al. [8]. It was shown that the carbon ions comprising a multiple hit were typically separated by less than 5 nm, when analyzing a low-alloyed steel. They also observed a strong crystallographic dependence on the positions of carbon ions from multiple events. The influence of crystallography on the field evaporation behavior of an Al-alloy was also studied by De Geuser et al. [9]. They concluded that the multiple events were caused by correlated evaporation, in particular at low-indexed poles. The possibility of extracting information from the multiple hit events has been investigated in detail by Saxey [10], who also observed molecular dissociation among the multiple hit events in GaN.

The detection efficiency of the system is an important parameter for the performance, and a high value is desired. However, the number of multiple hits and the number of ions detected in multiple hit events increases as the detection efficiency increases. In this paper we explore the possibility of deliberately decreasing the detection efficiency in order to decrease the fraction of multiple hits and its negative effect on concentration measurements.

2. Materials

Tungsten carbide (WC), which is known to be stoichiometric, was used to demonstrate the influence of the detection efficiency on the fraction of multiple hit events and on the carbon measurements. A duplex stainless steel (25Cr-9Ni-4Mo-0.23N-0.02C) and a hot-work tool steel (2.7Mo-1.7Cr-1.2V-0.38C) were also used to study the fraction of multiple hits. The samples were prepared by electropolishing and in the case of WC, final sharpening was performed using focused-ion beam milling.

3. Experimental Setup

The instrument used was an Imago LEAP 3000X HR. The ion detection system is based on a three-layer delay-line detector [11]. A multi-channel plate, with 60% open area, is located in front of the delay-line assembly. As the instrument is equipped with a reflectron lens, containing a grid that the ions pass twice, the detection efficiency ends up at 37%, according to the instrument supplier. The timing resolution is below 50 ps, but if ions hit close in space they have to be separated by more than 3 ns to be separated. In the best case, i.e when all ions are well separated in time and space, up to 15 ions can be recorded from a single pulse [12].

In order to decrease the detection efficiency, a grid was positioned behind the local electrode of the instrument. The grid was made of nickel and had a transmission (open area) of about 14%, a grid spacing of 12.5 μm and the square holes were 4.7 μm wide, see the SEM image in Figure 1. The grid was mounted to the standard electrode assembly (puck) in the following way, see Figure 2: First, the grid was cut in an 8×8 mm^2 square and glued (cyanoacrylate) to a Ø12 mm stainless steel plate, containing a Ø6 mm hole. Second, a 1.5 mm deep counterbore was machined at the exit opening of the puck. Third, the plate was glued to the puck, at the counterbore. In this way the grid was firmly affixed and could safely be handled inside the instrument. As a result, the grid was positioned about 7 mm behind the entrance of the local electrode. As changing electrode is a normal procedure, no further changes of the system were needed.

A previous experiment with a TEM grid having a 2 mm diameter opening, mounted at the same position as the 14%-grid, gave an image on the detector that had a diameter of half of the 38 mm detector diameter. We therefore conclude that the diameter of the image at the grid position is approximately 4 mm. Thus the image of the grid was magnified approximately 10X onto the detector. Field evaporated ions therefore reach the detector through a square array of holes with 125 μm spacing, or approximately 300 holes across the detector diameter. The detector area was consequently divided into around 72,600 small areas sensitive for ions. In a typical APT analysis of WC the analyzed area had a diameter of 50 nm. In such an experiment, the spacing between holes in the detector corresponds to 0.16 nm on the specimen surface, and each hole to a square 0.06 nm wide. Thus, even ion pairs (stemming from the same evaporation pulse) coming from (or appearing to come from) very closely positioned sites at the specimen surface will not pass the same hole, and the probability of recording both of these ions, given that one is detected, will decrease by 86%. If a too coarse grid would be used, most of the ions in pairs would either both pass the grid or both be stopped.

Analyses were made in both laser pulse mode (wavelength 532 nm) and voltage pulse mode. The pulse frequency was 200 kHz in all experiments. The WC was analyzed in laser mode with a pulse energy of 0.4 nJ and 0.35 nJ. The duplex steel and the tool steel were also analyzed in laser mode using a pulse energy of 0.3 nJ. The duplex steel was additionally analyzed in voltage pulse mode with a pulse fraction of 20%. The set temperature used for analyzing WC was 66 K and the steels were analyzed at 50 K. Analyses were performed on the same sample with and without the grid. For the experiments with the grid a local electrode with a 400 μm aperture was used, instead of a standard electrode with 40 μm aperture. The size of the aperture should not have any effect on the fraction of multiple events. The reason why using a larger aperture was merely that it is more robust, and does not suffer from degradation following specimen fracture, an effect that seems to be particularly severe for WC. The evaporation rate (expressed as the percentage of pulses generating ions) was decreased when the grid was used in order to compensate for the decrease in detection efficiency from 37% to 5%, in order to keep the evaporation conditions constant.

Data evaluation was performed using the software IVAS 3.6 and by examining exported epos-files, which contain information about the number of ions detected from each pulse, together with position and mass-to-charge ratio of each ion.

4. Results

In order to demonstrate the effect of using the grid on the fraction of multiple events, a set of materials and experimental parameters was used in analyses performed with the grid and without the grid. In each case the grid significantly decreased the fraction of multiple events, as shown in Table 1. As expected, the relative effect is larger when the fraction of multiples is high. It should also be noted that the mass resolution was unaffected by the grid. Furthermore, the appearance of the 3D reconstructions was not influenced, apart from the lower density of ions reflecting the lower detection efficiency. One analysis of WC contained a small region of Co-binder phase, and the interface appeared sharp and undistorted.

Henceforth, only the analysis of WC using a laser pulse energy of 0.35 nJ will be considered, as the WC analyzed using 0.40 nJ gave almost identical results, and as the steel analyses are much less affected by decreasing the detection efficiency. The carbon concentration was determined using standard procedures to 48.2 and 49.8 at.% from the analyses made without and with the grid, respectively. Hence, the measurement improved by a fair amount. The number of ions in the analyses was 880,000 and 300,000 without and with the grid, respectively, so the uncertainty from the counting statistics was negligible, as far as C and W are concerned. If only single events were included in the quantification, the carbon concentration became 43.8 at.% using the standard local electrode, whereas if the grid electrode was used the concentration increased to 49.2 at.%. The carbon concentrations obtained using only multiple events were 52.0 and 52.9 at.%, respectively. The distribution of ion types in the two analyses, divided into single and multiple events, is presented in Table 2. It is interesting to note that the different charge-states are not present in single and multiple events to the same extent. For example, in the analysis obtained with the standard local electrode, a clear majority of C^{+} is detected in multiple events, whereas C^{2+} is detected more often in single events than in multiple events. Regarding W, all ions except W^{4+} are mainly registered in single events. The only molecular ion of a significant amount containing W is WC^{3+}.

The relative frequency of events containing a certain number of ions is shown in Figure 3. As expected, many more events contain a large number of ions when using a standard local electrode. For example, when using the grid 0.3% of the ions came from events containing more than two ions. However, when using a standard local electrode almost 9% of the ions came from events containing more than two ions.

The distributions of distances between ions detected in multiple events containing two ions (pairs) obtained from analyses performed with and without the grid are shown in Figures 4-5. The pair distance ranges from about 1 to 10 nm, with a peak around 4 nm. The distances appear to be slightly longer in the distance distribution obtained with a standard local electrode, but this is most probably because the reconstruction parameters have not been correct in both cases. As the aperture of the grid local electrode is larger, the k-parameter is larger (k=V/(FR), where V is the

voltage, F is the evaporation field and R is the tip radius). In the present reconstructions k was set to 4 and 6, for the standard local electrode and the grid local electrode, respectively, and F was 40 V/nm. In fact, the pair distance distribution could perhaps be used for reconstruction calibration purposes, provided we understand the physics behind.

From Figures 4-5 it could be erroneously concluded that very short distances are not very common, as the number of pairs detected at distances decreases below about 3-4 nm. However, this effect comes largely from the fact that the pair distance probability density distribution p(r) is the pair distance distribution f(r) divided by $2\pi r\Delta r$, i.e. $p(r)=f(r)/(2\pi r\Delta r)$, where r is the distance and Δr is the differential increment of r. The probability density distributions are presented in Figures 6-7, and they indicate that the relative frequency does not decrease for short distances, at least not until below about 1 nm.

In figure 4, it can be seen that a vast majority of the detected pairs are W-C (84%), and that C-C pairs (10%) are more common than W-W pairs (2%). When analyzing the data further, it was found that out of the W-C pairs, 65% were C^{2+}-W^{3+}. The C-C pairs were almost exclusively C^{+}-C^{2+} (98%). The detector hit maps, as well as the reconstructions, obtained during analysis of WC contain almost no crystallographic features, and the hit maps made using single and multiple ions look similar. It is therefore supposed that crystallographic effects on the formation of multiple ions, as reported in refs. [8, 9], are marginal in this case.

5. Discussion

The quantification of WC is reasonably good when using the standard local electrode, considering the large fraction of multiple events. One reason for this is probably that most of the pairs are W-C, with ions arriving at the detector well separated in time. These ions should therefore be detected, and even if they are lost, it affects both C and W. The W-C pairs are also further apart on the detector than W-W and C-C pairs (see figures 6-7). The more or less complete absence of C^{+}-C^{+} and C^{2+}-C^{2+} pairs could be a consequence of the field evaporation process and the way molecular ions split [4, 10], but at least part of the explanation is that they are not both detected because of the dead time of the detector, and this is probably the main cause for the loss of C in the analyses.

An interesting observation is that the pair distance probability density distributions decrease when the distance becomes short. This behavior would be expected for pairs having the same mass-to-charge state ratio, because they arrive almost at the same time and would be missed because of the dead time. However, the same feature is present for all ions, including the W-C pairs. A possible interpretation would be that the ions largely evaporate as molecular WC ions, which are post-ionized (mainly to WC^{5+}) and then split (mainly to C^{2+}-W^{3+} pairs). In order to preserve the momentum perpendicular to the field direction, they drift apart a distance corresponding to a few nm on the specimen surface. The ions that are mostly separated are the W-C pairs and it is clear that a C^{2+} dissociating from a heavy W can obtain more motion perpendicular to the ideal trajectory than a C^{2+} dissociating from a light C.

The peak in the pair distance distributions of all pairs in Figure 4 is located around 4 nm, whereas W-W pairs have their peak at 1.5 nm and the C-C pairs at about 2 nm. This is similar to what was observed for C-C pairs in ref. [8]. However, the distances are much larger than what was observed for Al in ref. [9], where the peak was at about 0.7 nm. The main reason for this difference is probably that the field evaporation of Al occurs in a fashion that is close to ideal (despite the occurrence of correlated evaporation), giving a desorption map with much crystallographic information, and agrees with simulations. In the case of WC, on the other hand, the evaporation is less ideal. It is difficult to tell whether the multiple events are mainly caused by dissociation of molecules or correlated evaporation. Regardless of mechanism, it results in a spread of the ions, as it is highly unlikely that a W atom and a C atom sitting 4 nm apart on the sample would field evaporate on the same pulse.

Generally, the detection efficiency should be as high as possible, in particular when studying small clusters, segregation or elements of low concentration. On the other hand, if quantification of the major elements in a phase of reasonably large features (>50 nm) is the objective, a reduction in detection efficiency and thereby a reduction in the amount of multiple hit events, can significantly improve the result. The method presented here is a very simple way to reduce the detection efficiency. By studying the influence of the detection efficiency on the measurement, the part of a problem that is related to multiple events can be singled out. Hence, for all materials where the fraction of multiple events is high, the method presented here can function as a control experiment for establishing the influence of multiple events on the measured concentration. Once this is known, a normal electrode can be used for subsequent experiments, and the effect of the multiple events can be corrected for. A further approach would be to use a grid that covers half the image. Then the effect of the detection efficiency on the results could be observed in one analysis.

The effect of multiple hits on the quantification accuracy must be taken into account when developing detectors with detection efficiencies approaching unity. Already at a detection efficiency of 37% the effects can be significant, when using the current detector technology. If the detection efficiency is to increase much it is important to also improve the multiple hit performance of the detector, otherwise the improvement will in many cases not improve the accuracy of quantitative measurements, but rather the contrary. In order to detect two identical ions hitting the detector at the same position, the dead time must be very low, at least below 1 ns. In case the mass resolution is worse, the dead time could become less critical. However, the time spread of two identical ions originating from the same position and hitting the detector at the same position, is likely smaller than suggested by the overall mass resolution. Alternatively, the size of the detector area affected by a hit has to be much smaller (corresponding to 1 nm on the sample). It is unlikely that the delay line technology can achieve both high detection efficiency and excellent multiple hit capability (with maintained or improved mass resolution). Therefore, a new detector technology is indeed needed to reach the ultimate goal of 100% detection efficiency, unlimited multiple hit capability and further improved mass resolution. The situation would also improve if the detector pulse energy was measured. Not only would it be possible to separate different ions in the same peak

(eg. C_2^+ and C_4^{2+} at 24 Da), but also to measure the number of identical ions hitting the same position at the same time.

6. Conclusions

During atom probe tomography the dead time of the detector can result in a loss of certain elements when more than one ion from a single pulse hit the detector close in both time and space. Here it is shown that the effect can be significantly reduced by inserting a grid filter in the ion flight path. Although this decreases the detection efficiency, an improvement in carbon quantification was demonstrated when analyzing WC.

References

[1]. M. Thuvander, J. Weidow, J. Angseryd, L.K.L. Falk, F. Liu, M. Sonestedt, K. Stiller, H.-O. Andrén, Quantitative atom probe analysis of carbides, Ultramicroscopy 111 (2011) 604-608.

[2]. F. Tang, B. Gault, S.P. Ringer, J.M. Cairney, Optimization of pulsed laser atom probe (PLAP) for the analysis of nanocomposite Ti-Si-N films, Ultramicroscopy 110 (2010) 836-843.

[3]. T. Kinno, H. Akutsu, M. Tomita, S. Kawanaka, T. Sonehara, A. Hokazono, L. Renaud, I. Martin, R. Benbalagh, B. Sallé, S. Takeno, Influence of multi-hit capability on quantitative measurement of NiPtSi thin film with laser-assisted atom probe tomography, Appl. Surf. Sci. 259 (2012) 726-730.

[4]. M. Müller, B. Gault, G.D.W. Smith, C.R.M. Grovenor, Accuracy of pulsed laser atom probe tomography for compound semiconductor analysis, J. Phys.: Conf. Ser. 326 (2011) 012031.

[5]. G. Da Costa, F. Vurpillot, A. Bostel, M. Bouet, B. Deconihout, Design of a delay-line position-sensitive detector with improved performance, Rev. Sci. Instrum. 76 (2005) 013304.

[6]. J. Zackrisson, M. Thuvander, P. Lindahl, H.-O. Andrén, Atom probe analysis of carbonitride grains in (Ti, W, Ta, Mo)(C, N)(Co/Ni) cermets with different carbon content, Appl. Surf. Sci. 94-95 (1996) 351-355.

[7]. J. Angseryd, F. Liu, H.-O. Andrén, S.S.A. Gerstl, M. Thuvander, Quantitative APT analysis of Ti(C, N), Ultramicroscopy 111 (2011) 609-614.

[8]. L. Yao, B. Gault, J.M. Cairney, S.P. Ringer, On the multiplicity of field evaporation events in atom probe: A new dimension to the analysis of mass spectra, Philos. Mag. Lett. 90 (2012) 121-129.

[9]. F. De Geuser, B. Gault, A. Bostel, F. Vurpillot, Correlated field evaporation as seen by atom probe tomography, Surf. Sci. 601 (2007) 536-543.

[10]. D.W. Saxey, Correlated ion analysis and the interpretation of atom probe mass spectra, Ultramicroscopy 111 (2011) 473-479.

[11]. O. Jagutzki, A. Cerezo, A. Czasch, R. Dorner, M. Hattas, Min Huang, V. Mergel, U. Spillmann, K. Ullmann-Pfleger, T. Weber, H. Schmidt-Bocking, G.D.W. Smith, Multiple hit readout of a microchannel plate detector with a three-layer delay-line anode, IEEE Trans. Nucl. Sci. 49 (2002) 2477-2483.

[12]. R. Ulfig, D.J. Larson, T.F. Kelly, Personal communication.

Tables

Table 1. Fraction of ions detected in multiple events.

Material	Pulse mode	Pulse	Multiples (%) without grid	Multiples (%) with grid
Duplex Steel	Laser	0.30 nJ	4.3	2.2
Duplex Steel	Voltage	20%	27.6	7.0
WC	Laser	0.40 nJ	46.7	9.3
WC	Laser	0.35 nJ	46.4	9.6
Tool Steel	Laser	0.30 nJ	4.2	3.0

Table 2. Distribution (%) of atoms in the WC mass spectra divided into single events and multiple events, with a normal electrode and with the grid. The error bars represent ±2σ, from the counting statistics.

Ions	Normal electrode		Grid	
	Single	Multiple	Single	Multiple
C^{2+}	17.97 ± 0.08	17.55 ± 0.08	32.5 ± 0.2	3.78 ± 0.07
C^{+}	4.72 ± 0.05	7.09 ± 0.05	11.1 ± 0.1	1.47 ± 0.04
C_3^{2+}	0.012 ± 0.002	0.036 ± 0.004	0.027 ± 0.006	0.004 ± 0.002
C_2^{+}	0.057 ± 0.005	0.100 ± 0.007	0.37 ± 0.02	0.052 ± 0.008
W^{4+}	1.07 ± 0.02	2.53 ± 0.03	2.61 ± 0.06	0.51 ± 0.03
W^{3+}	24.46 ± 0.09	17.08 ± 0.08	36.1 ± 0.2	3.60 ± 0.07
W^{2+}	3.68 ± 0.04	3.24 ± 0.04	6.78 ± 0.09	0.67 ± 0.03
WC^{3+}	0.29 ± 0.01	0.124 ± 0.008	0.37 ± 0.02	0.056 ± 0.009
Total	52.2 ± 0.1	47.7 ± 0.1	89.9 ± 0.3	10.1 ± 0.1

Figure captions

Figure 1. SEM micrograph of the grid. The open area is about 14%, and the distance between the holes is about 12.5 μm.

Figure 2. Photo showing the local electrode assembly with the grid.

Figure 3. The relative frequency of events containing different number of ions, from WC analysis with and without grid, respectively.

Figure 4. Pair distance distributions from analysis of WC using a standard local electrode.

Figure 5. Pair distance distributions from analysis of WC using the grid local electrode.

Figure 6. Pair distance probability density distributions from analysis of WC using a standard local electrode.

Figure 7. Pair distance probability density distributions from analysis of WC using the grid local electrode.

Figure 1.

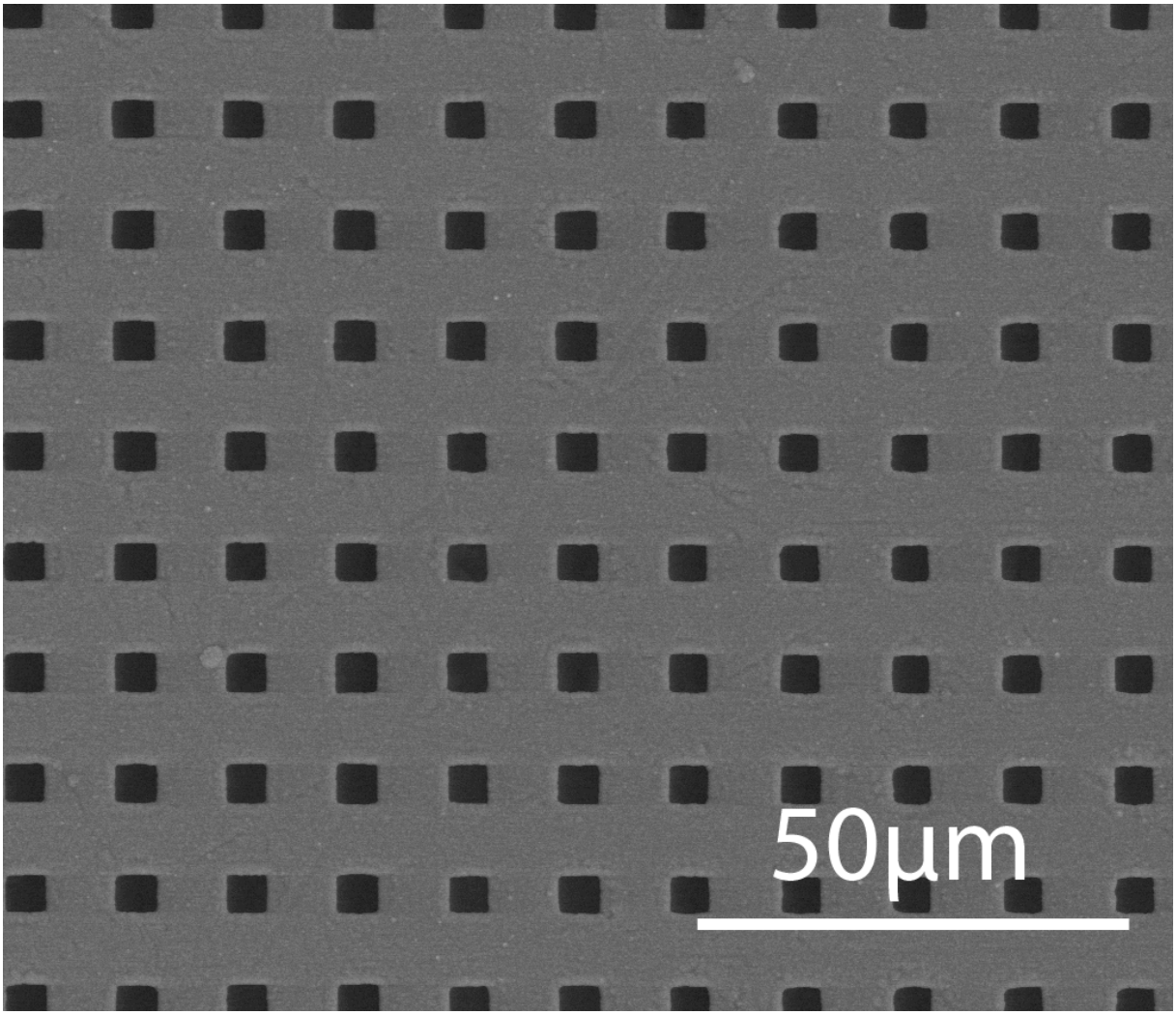

Figure 2.

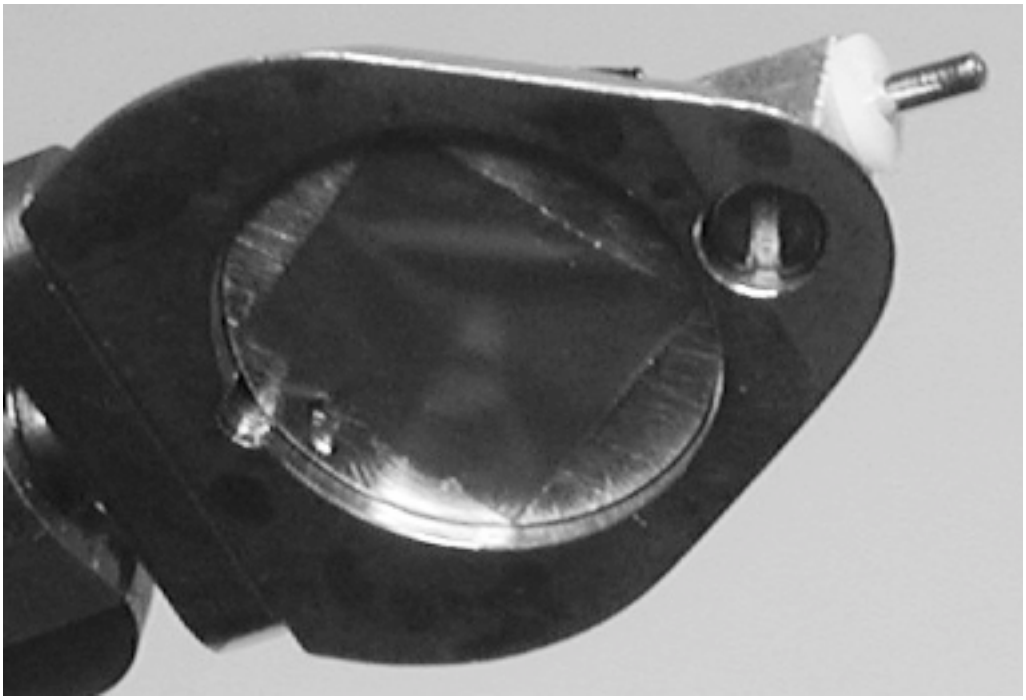

Figure 3.

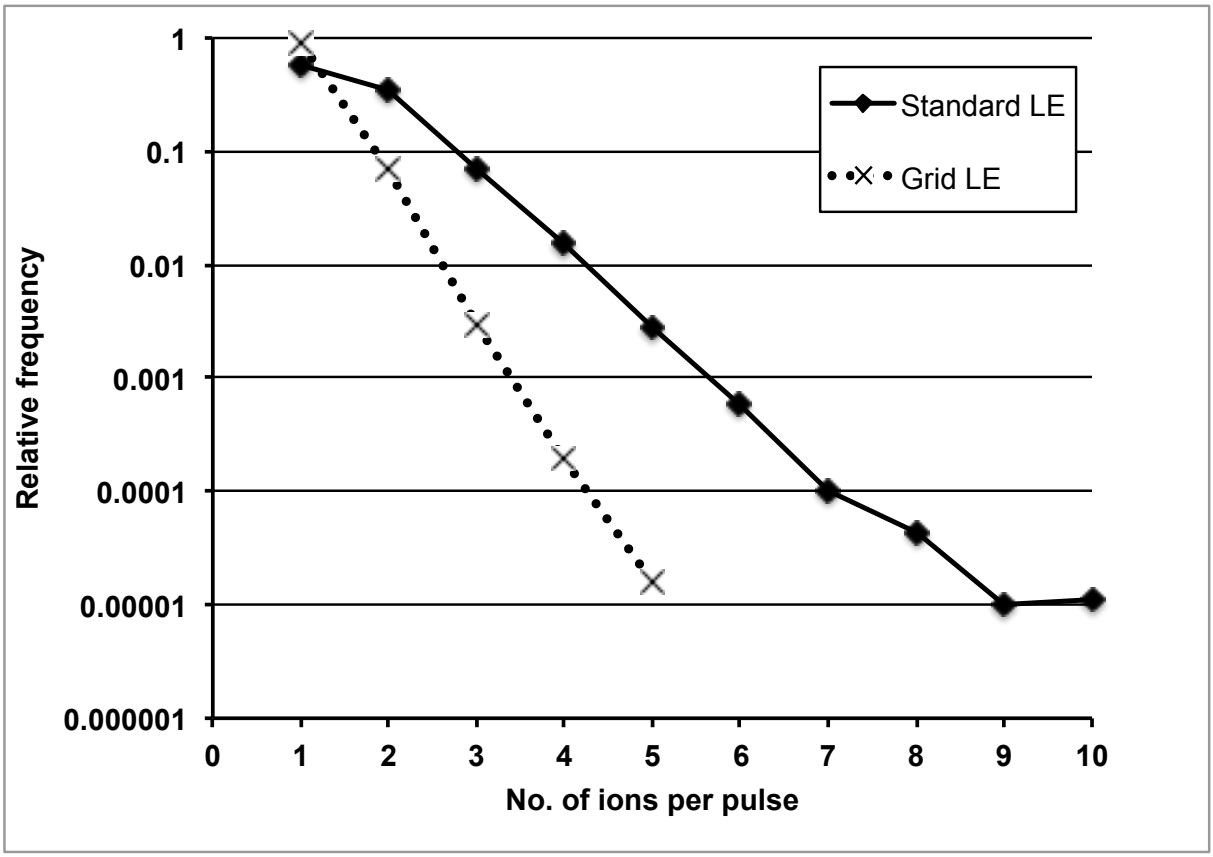

Figure 4.

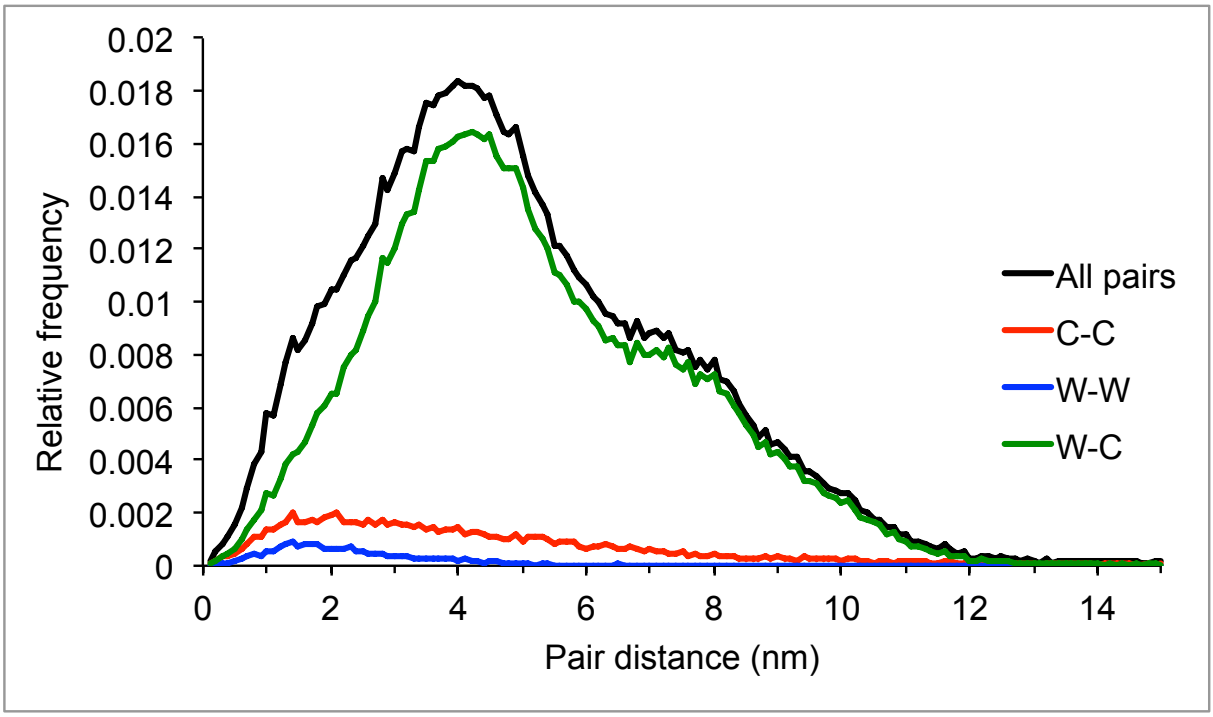
0.02
0.018
0.016
0.014
0.012
0.01
0.008
0.006
0.004
0.002
0
Relative frequency
0
2
4
6
8
10
12
14
Pair distance (nm)
All pairs
C-C
W-W
W-C

Figure 5.

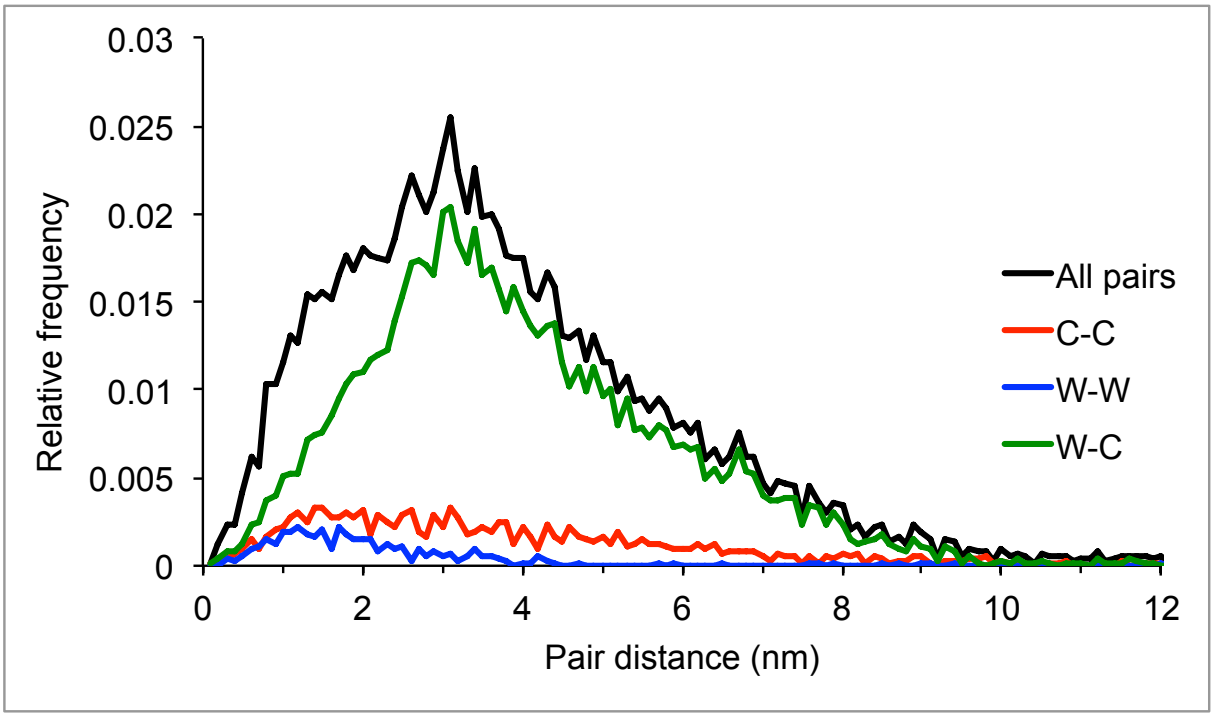
0.03
0.025
0.02
0.015
0.01
0.005
0
Relative frequency
0
2
4
6
8
10
12
Pair distance (nm)
All pairs
C-C
W-W
W-C

Figure 6.

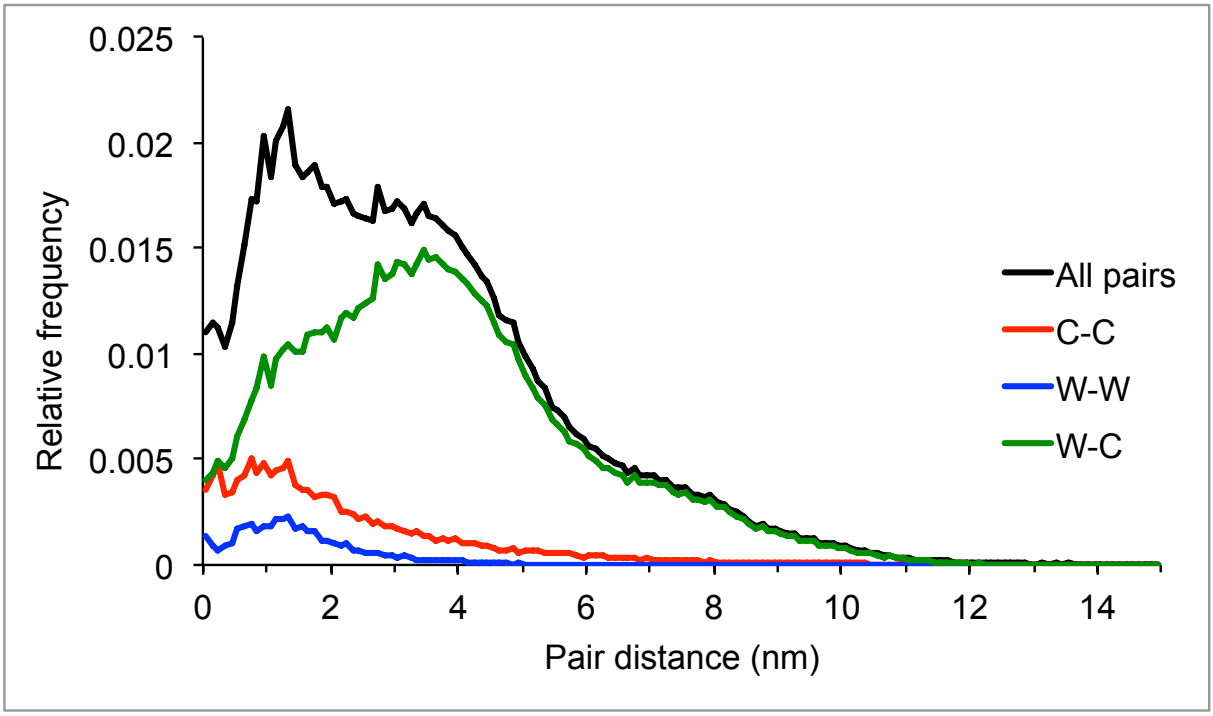
0.025
0.02
0.015
0.01
0.005
0
Relative frequency
0
2
4
6
8
10
12
14
Pair distance (nm)
All pairs
C-C
W-W
W-C

Figure 7.

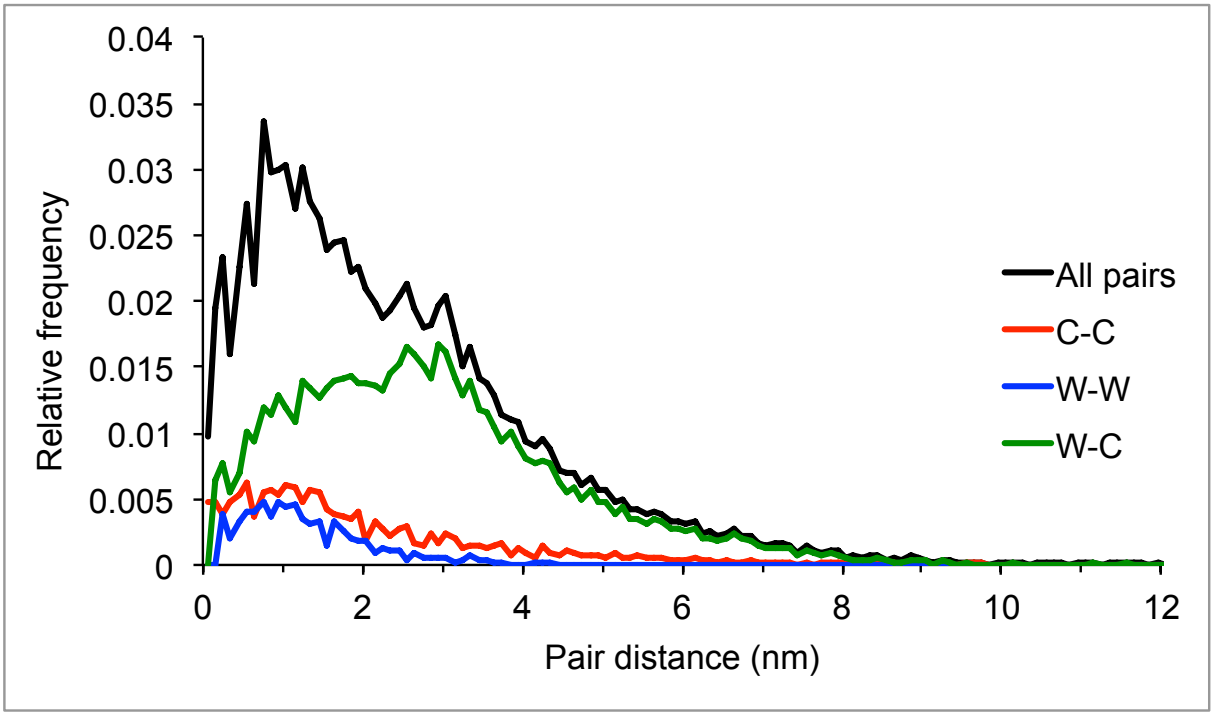
0.04
0.035
0.03
0.025
0.02
0.015
0.01
0.005
0
Relative frequency
0
2
4
6
8
10
12
Pair distance (nm)
All pairs
C-C
W-W
W-C